

Design of Azimuth Altitude Dual Axis Tracker (AADAT) Based Photo Voltaic System and its Comparison with Based Photo Voltaic Systems.

G.ANANTH RAM, DR. M.GOPI CHAND NAIK.

P.G. Student ,Dept. of Electrical Engineering

Associate Professor, Dept. of Electrical Engineering, Andhra University College of Engineering (A), India

-----***-----

Abstract- Solar energy is radiant light and heat from the sun that is harnessed using a range of ever evolving technologies such as solar heating, concentrated solar power, concentrator photovoltaics, solar architecture and artificial photosynthesis. To produce the maximum amount of energy, a solar panel must be perpendicular to the light source. Because the sun moves both throughout the day as well as throughout the year, a solar panel must be able to follow the sun's movement to produce the maximum possible power. The solution is to use a tracking system that maintains the panel's orthogonal position with the light source. This paper aims at designing Azimuth Altitude Dual Axis Tracker (AADAT) based photovoltaic system and to test the change in its angular position w.r.t the sun, the comparison of the dual axis system with various other tracker systems is simulated and the energy generated over a range of latitudes is also simulated. The simulation results are shown in this paper.

Key Words: Dual axis, photovoltaic cell, solar tracking, photo sensor, microcontroller.

1.INTRODUCTION

1.1 Solar Tracking

The Sun travels through 360 degrees east to west per day, but from the perspective of any fixed location the visible portion is 180 degrees during an average 1/2 day period. A solar panel in a fixed orientation between the dawn and sunset extremes will see a motion of 75 degrees to either side. Rotating the panels to the east and west can help recapture those losses. A tracker rotating in the east-west direction is known as a single-axis tracker. [1]

The Sun also moves through 46 degrees north and south during a year. The same set of panels set at the midpoint between the two local extremes will thus see the Sun move 23 degrees on either side. A tracker that accounts for both the daily and seasonal motions is known as a dual-axis tracker. There are two types of dual axis trackers, they are:

- Tip-Tilt Dual Axis Trackers.(TTDAT)
- Azimuth-Altitude Dual Axis Trackers.(AADAT)

1.2 AADAT System

AADAT has its primary axis (the azimuth axis) vertical to the ground. The secondary axis, often called elevation axis, is then typically normal to the primary axis. AADAT systems can use a large ring mounted on the ground with the array mounted on a series of rollers. The main advantage of this arrangement is the weight of the array is distributed over a portion of the ring. This allows AADAT to support much larger arrays. AADAT offers increase of electrical power gains up to 43.87% for the two axes, 37.53% for the east-west, 34.43% for the vertical and 15.69% for the north-south tracking. [2]

2. DESIGN

The AADAT system can be divided into two parts as electrical and mechanical. The electrical system consists of four PV sensors which provide feedback to a microcontroller. This microcontroller processes the sensor input and provides output to two H-Bridges and four LED indicators. The entire electrical system is powered by rechargeable batteries. The H-bridge controls two DC motors, which are also part of the mechanical system. The mechanical system also contains two worm gear assemblies that adjust the PV sensors. The voltage rating of the generator considered for this was 12V and the gear ration of the worm gear system was 180:1.

2.1 H-Bridge

The electrical system has two H-Bridges, the circuit is modified for the reasons: improved efficiency, lower probability of faults, reduction of losses due to heat dissipation, surges and improved performance. The modified H-Bridge Circuit is as shown in Fig -1.

2.2 Solar Sensor Array

To provide an accurate and reliable tracking of the sun, a solar sensor array is designed. The solar sensors are primarily chosen based on linearity of the output response due to the change in the angle of incidence. The sensor tilt angle is chosen that obtained the highest angular response. The polycrystalline photovoltaic cells have the flattest response with near constant sections. Hence, two

polycrystalline photovoltaic sensors tilted at 25° are used for both the azimuth and altitude axis.[3],[4],[5].

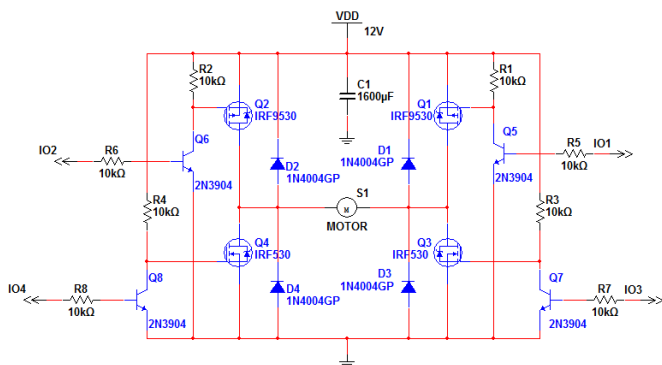


Fig -1: Modified H-Bridge Schematic.

2.3 Analog Comparator Circuit

To provide an interface from the solar sensors to the H-bridge, a circuit that compares the voltage of two photosensors and outputs a control signal to each of the four MOSFET inputs of the H-bridge is to be designed. This circuit design need to accurately sense the voltage difference between the photosensors and provide reliable inputs to the H-bridge. The first section of this circuit, that detects the voltage difference, is composed of an analog comparator circuit. The second section, that provides the control inputs to the H-bridge, consists of logic gates.

Two photosensors are used in the circuit as mentioned above. In order obtain a voltage that depended on the resistance change of the photosensor, a voltage divider is designed. This voltage divider is supplied by 5 V, due to convenience. A 100 kΩ potentiometer is used to complete the voltage divider. At the output a 51 kΩ resistor is used for current protection. Two Op-amps are connected to the two sensor voltage dividers and configured in the no-feedback, comparator setup. The circuit is further modified to make the setup less bulky.

As mentioned earlier the H-bridge requires accurate control inputs to each of the four MOSFETs. However, the above constructed comparator only provides two inputs, thus a set of logic gates are used to obtain the four inputs. When the comparator outputs two high signals, which corresponds to the tracker being pointed at the light source, outputs to the P-channel MOSFETs on the bridge need to go low and the outputs to the N-channel MOSFETs need to go high. If one sensor shows a higher light intensity, the corresponding output goes high. The logic circuit needs to send a signal to the H-bridge to turn on the P-channel and N-channel MOSFETs that correspond to rotation the system in the direction of the light. The reverse goes for the opposite sensor. Finally, when both sensors output a low value, which is impossible, but still needed to be planned for, the H-bridge needed to be shut off in the same fashion as when the sensors outputs are both high. The truth table for the logic needed in

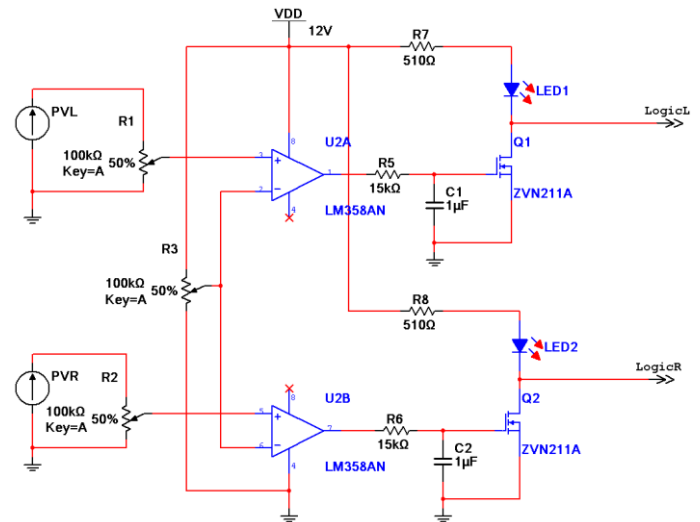


Fig -2: Comparator Circuit.

is Table 1. Outputs 1 and 2 correspond to the P-channel input and Outputs 3 and 4 go to the N-channel inputs. Output 1 and 3 go to the same side of the H-bridge and 2 and 4 go to the other side. The logic Circuit and truth table are shown below.

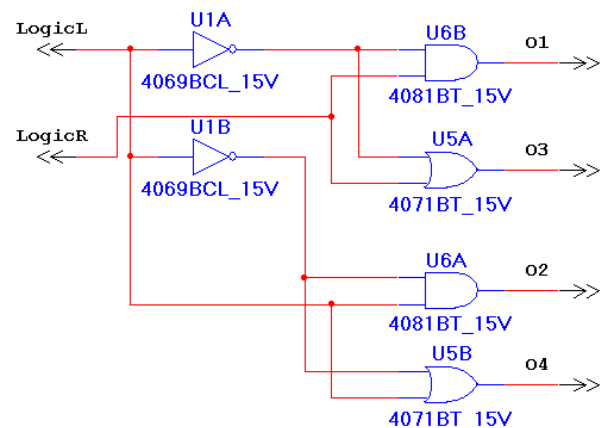


Fig -3: Logic Schematic

Sensor L	Sensor R	Output 1	Output 2	Output 3	Output 4
0	0	0	0	1	1
0	1	1	0	0	1
1	0	0	1	1	0
1	1	0	0	1	1

Table -1: Comparator Logic

2.4. Digital Comparator Circuit

Because of the drawbacks present in the analog control system, a microcontroller-based, digital control system is considered. The microcontroller allowed a minimal control

circuit complexity, reduced power consumption and allowed for additional features to be introduced in the tracker.

The microcontroller selected has at least four analog-to-digital converter (ADC) inputs to take the four signals from the four sensors. It also has a minimum of eight digital outputs, four for both of the motor H-bridges. Finally, the microcontroller has very low power consumption when active to keep the efficiency as high as possible. The microcontroller is either AVR or PIC microcontroller.

The microcontroller's function is to compare the voltage levels of the two sensors for one axis of rotation and send the appropriate signal to the H-bridge to move the motor in a certain direction. To reduce the amount of jitter the system has, the microcontroller takes the two voltage values of the sensors and finds the difference between the two. The difference is compared to some reference value. If it is greater than the positive reference value, the microcontroller sends a signal to the H-bridge to move the tracker in one direction. If the difference is less than the negative reference, the microcontroller sends a signal to move the tracker in the opposite direction. Setting the reference to zero will reduce the error to the minimum but it will also introduce significant jitter when a shadow passes over the sensors. Setting the reference to a value greater than zero allows some hysteresis into the tracker but also increases the error. Setting the reference, for example, to 5 means there is a maximum allowable difference between the two sensors of $5 \times 4.88\text{mV} = 24.4\text{mV}$. Solving for the difference in angle between the tracker and the sun, this voltage difference corresponds with an angular difference of 0.9945° which is a 0.553% allowable error.

Additionally, the microcontroller examines the voltage outputs of the sensors in relation to night-time conditions. If the values correspond to those during nighttime, the tracker will shut everything off except for the microcontroller to decrease power consumption. This also avoids the problem of the tracker focusing on a nearby nighttime light source such as a streetlamp or building.

2.5 Simulation and Results

The first part of the simulation was to collect the specifications of the system. The major portion of the simulation would rely on an accurate representation of how the sensors act during the day. The final panels used had an approximate maximum open circuit voltage of 1.44V as verified through testing. The angle between the backs of the panels is 25° which means that the angle between the normal to the faces of the panels, denoted as gamma (γ), is 155° . If the angle of the sun to some reference point denoted as alpha (α), the voltage across one solar panel can be ideally represented in an equation:

$$V_{PV1} = 0.72 \cos(\alpha + \gamma/2) + 0.72V \quad (1)$$

$$V_{PV1} = 0.72 \cos(\alpha + 77.5^\circ) + 0.72V \quad (2)$$

Inversely, the voltage across the opposing panel can be ideally represented as:

$$V_{PV2} = 0.72 \cos(\alpha - 77.5^\circ) + 0.72V \quad (3)$$

Because cosine is an even function, the voltage difference between the two panels will be zero at $\alpha = 0^\circ$. To incorporate the angular position of the tracker (p) according to the same reference point as the sun, the equations were modified to be:

$$V_{PV1} = 0.72 \cos((\alpha - p) + 77.5^\circ) + 0.72V \quad (4)$$

$$V_{PV2} = 0.72 \cos((\alpha - p) - 77.5^\circ) + 0.72V \quad (5)$$

Now given an angle of the sun and the tracker, the voltage across the panels can be calculated.

Second, the speed of the motor had to be calculated. Putting the motor under load and changing the PWM amounts, the slowest effective speed as at approximately 17% duty cycle. [6] Any slower and the motor could not move the tracker. The measured speed at 100% duty cycle was 5098.2 rpm or 530.74 rad/s. Given the duty cycle and the gear reduction ratio of 180:1, the speed of the tracker is approximately 0.5203 rad/s.

For the simulation, five vectors were created. The first vector is the time vector to show the transient nature of the system. The second is the vector that denotes the angular position of the sun over the duration of the time vector. The rate at which the sun changes its position can be roughly calculated as 360° in a day or 7.272×10^{-8} rad/ms. The position vector is initially set at the reference point and is modified as the simulation progresses. The last two vectors are for the voltages of the panels over time. Each one is calculated from the present value of the sun and the position of the tracker.

The simulation runs the changing sun position through the solar panel equations to get the voltages on the panels at the current position. Simulating the microcontroller, the difference between the two voltages is compared to some reference value that can be changed. If the difference is greater than the reference or less than the negative reference, the simulation increments the position vector at the rate of the tracker speed, 0.5203 rad/s in the direction correspond to which sensor is getting more radiation. If the difference is in between the positive and negative values of the reference, the position is maintained.

After then simulation has run for the specified amount of time, one last vector is created as an error vector. The error is the difference between the sun and the tracker. This vector was converted into degrees for readability.

Using the reference of $5 * 4.88\text{mV} = 24.4\text{mV}$, gamma in radians which is 2.7053 rad and the speed of 0.5203 rad/s, the simulation plots the voltages on the panels, the position of the sun and the tracker next to each other as well as the error of the tracker all over 500 seconds.

In Fig -5 the zoomed in graphs show the tracker jumps in position approximately every 7 seconds. This is a result of the tracker forming a "safe zone" that is 0.9945° off of the sun's position. When the tracker is within this safe zone, the system is at equilibrium and the tracker does not move.

When the sun moves outside of the safe zone, the tracker sees the error and responds by turning the motor on in that direction. The motor spins the tracker back into the safe zone and is moving faster than the tracker can respond so it moves it to approximately 0.965° from the sun, well within the safe zone. The tracker then is at equilibrium until the sun moves too far again and the cycle repeats.

To examine the inner workings of the tracker, it is best to also look at how the panel voltages are reacting over time. Modifying the simulation code to output the solar panel voltages as well as the difference between the two over an interval of 15 seconds, the result is Fig -7.

Panel 1 is the sensor that is closest to the sun during this simulation. If the direction of the sun's movement is reversed, Panel 2 would be the closer. Therefore the simulation is correct in showing that as the sun moves, the voltage on Panel 1 is increasing and the voltage on Panel 2 is decreasing. The difference between these two slowly increases until it reaches 24.4mV at which point the tracker begins to move. The stepped results are still an effect of the motor speed described above.

The total solar radiation at a place is considered and the response in form absorption of radiation while using various tracking mechanisms is observed and the energy generated over a range of latitudes is also observed. This is achieved by giving the input latitude of a desired location and the index of time for which the corresponding radiation should be simulated. The results are shown in Fig -8 and Fig -9 given below.

Fig -8 clearly shows that the dual-axis tracking system, despite its error, is absorbing almost all the available light. The X-axis tracking seems to be the better tracking system at the beginning of the day, when the sun is first rising but after a few hours it falls behind the radiation absorbed by the Y-axis. This is because the X-axis still suffers from the fact that it is pointed towards the zenith in the Y direction and will never be able to achieve the high percent absorption that the Y-axis benefits from at noon. Finally, the immobile tracker clearly has the least amount of absorption as it cannot compensate for its error in either direction.

The final part of the functionality testing of the tracking system is to compare its performance to other types of panel orientations and tracking systems. To do this, an accurate simulation of the sun's angle to particular point on the earth's surface was needed to calculate the power and energy gained by a tracking system.

To simplify the math, a few assumptions were made. One is that the earth is perfectly spherical so that elevation of the solar panel setup does not come into play. Second is assuming that the sun moves from exactly east to exactly west every day of the year. Finally, that the year is exactly 365, 24 hour days or 8760 hours long. Finally, that the time at the point of the solar panel corresponds to the sun's

position so that at midnight the sun is exactly behind the earth at 180° to the zenith and that at noon, the sun is directly between the east and west horizons or 0° to the zenith.

Given that the earth rotates a full 360° in 24 hours in an east-to-west direction, the following equation can be given for the angle of the sun to the zenith of the point on the earth given in the east-west direction henceforth called the X direction:

$$Z_x = 15^\circ (t - 12) \quad (6)$$

The variable t is the amount of time from midnight on the first day of the simulation in hours. This equation gives the following results:

$$t = 0 \text{ hours (midnight first day), } Z_x = 15^\circ(-12) = -180^\circ$$

$$t = 12 \text{ hours (noon first day), } Z_x = 15^\circ(0) = 0^\circ$$

$$t = 24 \text{ hours (midnight second day), } Z_x = 15^\circ(12) = 180^\circ$$

$$t = 36 \text{ hours (noon second day), } Z_x = 15^\circ(24) = 360^\circ = 0^\circ$$

And the cycle repeats every day.

To find an equation for the sun in the north-south direction, henceforth referred to the Y direction, the tilt of the earth's axis to its orbit around the sun is given at 23.5° . So as the earth orbits around the sun, the equator's Y angle to the sun goes from 0° at the vernal equinox to 23.5° at the summer solstice back to 0° at the autumnal equinox then to -23.5° at the winter solstice and finally back to 0° at the vernal equinox again. Given that this value fluctuates over the 365 day or 8760 hour year, the angle to the zenith on the equator is given as:

$$Z_{\text{equator}} = 23.5^\circ \sin(2\pi t/8760) \quad (7)$$

The time variable t is now the measure of hours from the midnight on the vernal equinox. However, because the point chosen might not be at the equator, the latitude also comes into effect. Positive latitude is the angle of the point specified on the earth's surface north of the equator. Negative latitude is consequently south of the equator. So to bring the latitude into the equation, ZY is now the difference of the latitude angle, defined as Φ , to the angle of the sun to the equator:

$$Z_y = \Phi - 23.5^\circ \sin(\pi t/4380) \quad (8)$$

Now that equations for the X and Y angle of the sun to the zenith of some point on the earth have been derived, the amount of available sunlight radiation to that point can be calculated. NASA defines this amount of radiation under perfectly sunny and clear conditions to be a function of the cosine of the angle of the sun to the zenith. So the radiation percent coming from both individual directions is defined as:

$$R_x = \cos(Z_x) = \cos(15^\circ (t - 12)) \quad (9)$$

$$R_y = \cos(Z_y) = \cos(\Phi - 23.5^\circ \sin(\pi t/4380)) \quad (10)$$

And then the total radiation of the sun hitting a point on the earth's surface at latitude Φ at time t in hours from midnight on the vernal equinox is:

$$R_T = R_x * R_y = \cos(15^\circ (t - 12)) * \cos(\Phi - 23.5^\circ \sin(\pi t/4380)) \quad (11)$$

To calculate the percent radiation absorbed by the solar tracking system, several observations are made about the movement of the tracker. The first is that the tracker will always be following the sun slightly behind its actual position by a maximum of 1.5° in both directions as verified by the measurements. Taking the cosine of this angle shows

that the tracker will be able to absorb 99.97% of all available light in one direction. For both directions, this value is squared bringing the percentage to 99.93% of all available radiation in both directions. Second is that aside from this error, the tracker will always orient any solar panel on it perpendicular to the sun in perfectly clear conditions.

Therefore, based on these assumptions the radiation absorbed by a panel mounted on this tracking system will be 99.93% of the total radiation meaning that the equation for this value over time will be:

$$P_{DT} = 0.9993 * R_{Total} \tag{12}$$

$$P_{DT} = 0.9993 * \cos(15^\circ (t - 12)) * \cos(\Phi - 23.5^\circ \sin(\pi t / 4380)) \tag{13}$$

Before plotting the equation for the dual tracker system over time, equations for several other systems needed to be derived for comparisons. The first being the tracker that only tracks in the east-west or X direction which is also referred to as a Horizontal Single Axis Tracker (HSAT) as discussed in Chapter 2. First, assuming the HSAT uses the same tracking system as the dual axis tracker, the tracking angle will lag slightly behind the sun by 1.5° over the course of a day. This means in the X direction, the HSAT can only absorb 99.97% of the radiation available. Second the HSAT will be oriented in the Y direction so it is pointed towards the zenith. Therefore, the HSAT percentage absorbed will also rely on the angle of the sun in the Y direction which it cannot compensate for. The absorption percent will be affected the cosine of Z_Y which brings the total equation to:

$$P_{XT} = 0.9997 * \cos(Z_X) * R_{Total} \tag{14}$$

$$P_{XT} = 0.9997 * \cos^2(15^\circ (t - 12)) * \cos(\Phi - 23.5^\circ \sin(\pi t / 4380)) \tag{15}$$

Tracking can also be done in the Y direction. This is usually done by using an immobile panel and varying its degree to zenith over the year to keep the sun's angle to the panel minimal without any mechanics. To simplify the mathematics and make the comparisons more relevant, two things are assumed. First, the tracker, man or machine, has the same amount of error in the Y direction as the HSAT tracker has in the X direction which is 99.97%. Second the panel is oriented in the X direction towards the zenith in the same way that the HSAT is oriented in the Y direction. Therefore, the Y direction tracker percentage absorbed will also rely on the angle of the sun in the X direction which the tracker cannot compensate for. The absorption percent will be affected the cosine of Z_X which brings the total equation to:

$$P_{YT} = 0.9997 * \cos(Z_Y) * R_{Total} \tag{16}$$

$$P_{YT} = 0.9997 * \cos(15^\circ (t - 12)) * \cos^2(\Phi - 23.5^\circ \sin(\pi t / 4380)) \tag{17}$$

The final panel orientation to be compared is the immobile panel orientation. This is assuming that the panel is placed perfectly level with the ground so that the panel's normal is perfectly oriented to the zenith. Therefore the percent of radiation absorbed with an immobile panel will be a function of the angle of the sun in both directions. This value will be determined by the cosines of both Z_X and Z_Y which brings the equation to:

$$P_{YT} = \cos(Z_X) * \cos(Z_Y) * R_{Total} \tag{18}$$

$$P_{YT} = \cos^2(15^\circ (t - 12)) * \cos^2(\Phi - 23.5^\circ \sin(\pi t / 4380)) \tag{19}$$

After deriving all four equations, they were used in MATLAB to create vectors over time during the day of the vernal equinox. The corresponding results are shown below in Fig - 7 and Fig - 8.

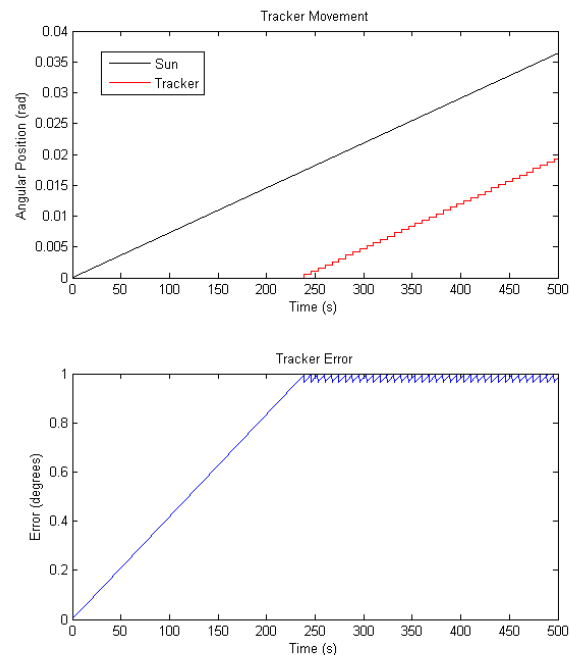


Fig -4: Simulation Results over 500 seconds

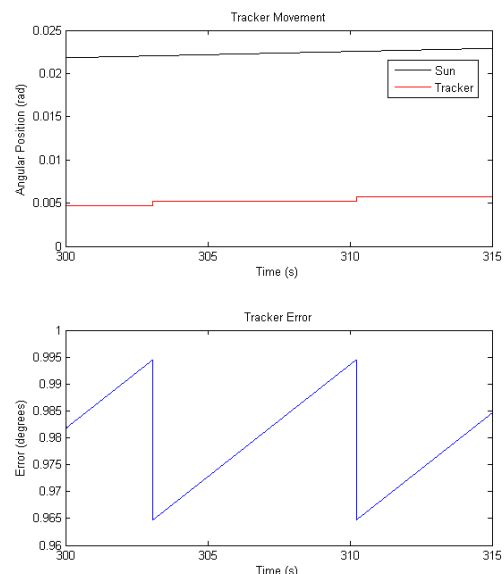


Fig -5: Simulation Results over 15 Seconds

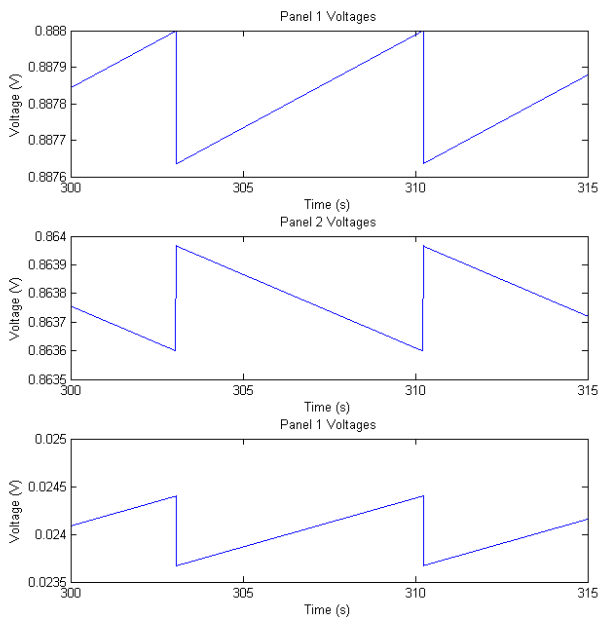


Fig -6 Simulation Panel Voltages over 15 seconds

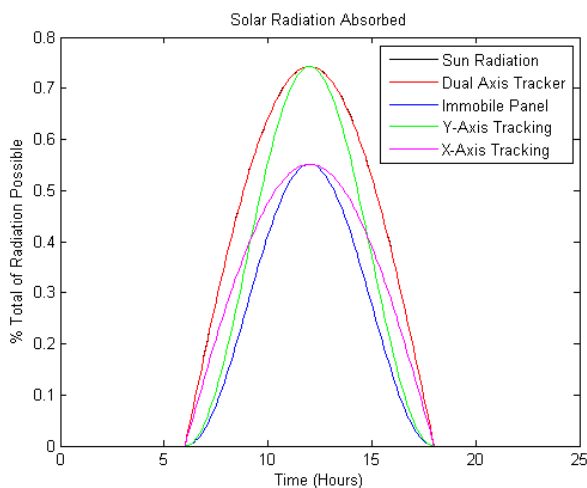


Fig -7: Total Solar Radiation vs Time Curve for various tracking mechanisms

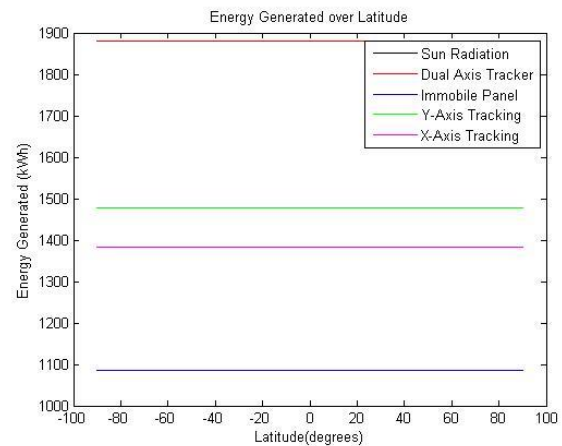


Fig -8: Energy Generated Over a Particular Latitude for Various Trackers

3 CONCLUSIONS

The Azimuth-Altitude Dual-Axis Solar tracker designed and built in this project show a clear benefit over both immobile and single-axis tracking systems. The tracker built has a maximum angular error to the sun of 1.5° in both axes of movement. This value corresponds to a 49% energy gain over an immobile solar panel setup assuming the solar panels mounted on the tracker and the immobile system are identical 20W panels. Furthermore, the single-axis trackers had gains over the immobile system for the entire range of latitudes but these gains were still lower than the dual-axis tracker for all latitudes.

REFERENCES

- [1] Mousazadeh, H., Keyhani, A., Javadi, A., Mobli, H., Abrinia, K., Sharifi, A. "A review of principle and sun-tracking methods for maximizing solar systems output". Renewable and Sustainable Energy Reviews.
- [2] .Roth, P., Georgiev, A., Boudinov, H.. "Cheap two Axis sun Following Device". Energy Conversion and Management. 2005.
- [3] Krauter, Stefan. "Solar Electrical Power Generation: Photovoltaic Energy Systems". Springer. 2006
- [4] Ackermann, T., Andersson, G., Söder, L. "Distributed generation: a definition". Electric Power Systems Research.
- [5] Mehleri, E., Zervas, P., Sarimveis, H., Palyvos, J., Markatos, N.. "Determination of the optimal tilt angle and orientation for solar photovoltaic arrays". Renewable Energy
- [6] Hamilton, R. "DC Motor Brush Life". IEEE Transactions on Industrial Applications. 2000.